

MODIS ATMOSPHERIC PROFILE RETRIEVAL ALGORITHM THEORETICAL BASIS DOCUMENT

W. PAUL MENZEL¹ and LIAM E. GUMLEY²

University of Wisconsin-Madison

1225 W. Dayton St.

Madison, WI 53706

Version 3

September 3, 1996

¹ NOAA/NESDIS (Internet: paul.menzel@ssec.wisc.edu)

² Cooperative Institute for Meteorological Satellite Studies (Internet: liam.gumley@ssec.wisc.edu)

TABLE OF CONTENTS

1. Introduction	1
2. Overview and background information	2
2.1 Objectives	2
2.2 History	2
2.3 Instrument Characteristics	3
3. Algorithm Description	6
3.1 Theoretical Background	6
3.1.1a Statistical Regression Profile Retrieval	7
3.1.1b Physical Profile Retrieval	9
3.1.2 Total Column Ozone	13
3.1.3 Total Column Precipitable Water Vapor	17
3.1.4 Atmospheric Stability	20
3.1.5 Estimate of Errors	21
3.2 Practical Considerations	21
3.2.1 Radiance Biases and Numerical Considerations	21
3.2.2 Data Processing Considerations	22
3.2.3 Validation	23
3.2.4 Quality Control	24
3.2.5 Exception Handling	24
3.2.6 Data Dependencies	25
3.2.7 Output Product Description	25
4. Assumptions	27
5. References	28

1. Introduction

The purpose of this document is to present an algorithm for retrieving vertical profiles of atmospheric temperature and moisture from multi-wavelength emitted thermal radiation measurements in clear skies. While the MODIS is not a sounding instrument, it does have many of the spectral bands found on the High resolution Infrared Radiation Sounder (HIRS) currently in service on the polar orbiting NOAA TIROS Operational Vertical Sounder (TOVS). Thus it will be possible to generate profiles of temperature and moisture as well as total column estimates of precipitable water vapor, ozone, and atmospheric stability from the MODIS infrared radiance measurements. These parameters will be used to correct for atmospheric effects for some of the MODIS products (such as sea surface and land surface temperatures, ocean aerosol properties, water leaving radiances, photosynthetically active radiation, ...) as well as to characterize the atmosphere for global greenhouse studies. The algorithms will be adapted from those used for the operational HIRS and GOES sensors, with adjustments to accommodate for the absence of stratospheric sounding spectral bands and to take advantage of the greatly increased spatial resolution (1 km MODIS versus 17 km HIRS) with good radiometric signal to noise (less than 0.35 C for typical scene temperatures in all spectral bands).

In this document we begin with a review of temperature and moisture retrieval algorithms, and an overview of the MODIS instrument specifications, followed by a description of the theoretical basis of the retrieval algorithm to be used for MODIS. This is followed by a discussion of the practical aspects of the algorithm implementation, and an outline of the planned validation approach.

2. Overview and background information

The purpose of this document is to provide a description of the theoretical and practical aspects of the temperature and moisture retrieval algorithm we are developing for MODIS. Most of the sounding expertise for this endeavor has been acquired with existing infrared sounding instruments, so this document necessarily focuses on results and experience from these sensors. The techniques developed for existing sensors will, we believe, translate directly to the MODIS instrument.

2.1 *Objectives*

The objective of this work is to develop an operational algorithm for retrieving vertical profiles (soundings) of temperature and moisture, total column ozone burden, total column precipitable water vapor, and several atmospheric stability indices from clear sky radiances measured by MODIS. The methods presented here are based on the work of Smith et al. (1985), and more recent similar work by Smith and Woolf (1988) and Hayden (1988). The clear advantage of MODIS for this task is the combination of spectral channels suitable for sounding and spatial resolution suitable for imaging (1 km at nadir). Temperature and moisture profiles at MODIS spatial resolution are required by a number of other MODIS investigators, including those developing sea surface temperature and land surface temperature retrieval algorithms. Total ozone and precipitable water vapor estimates at MODIS resolution are required by MODIS investigators developing atmospheric correction algorithms. The combination of high spatial resolution sounding data from MODIS, and high spectral resolution sounding data from AIRS, will provide a wealth of new information on atmospheric structure in clear skies. Cloud filtering will be achieved with the aid of the cloud mask product (ATBD MOD-06).

2.2 *History*

Inference of atmospheric temperature profiles from satellite observations of thermal infrared emission was first suggested by King (1956). In this pioneering paper, King pointed out that the angular radiance (intensity) distribution is the Laplace transform of the Planck intensity distribution as a function of the optical depth, and illustrated the feasibility of deriving the temperature profile from the satellite intensity scan measurements. Kaplan (1959) advanced the temperature sounding concept by demonstrating that vertical resolution of the

temperature field could be inferred from the spectral distribution of atmospheric emission. Kaplan noted that observations in the wings of a spectral band sense deeper regions of the atmosphere, whereas observations in the band center see only the very top layer of the atmosphere, since the radiation mean free path is small. Thus by properly selecting a set of sounding spectral channels at different wavelengths, the observed radiances could be used to make an interpretation of the vertical temperature distribution in the atmosphere.

Wark (1961) proposed a satellite vertical sounding program to measure atmospheric temperature profiles, and the first satellite sounding instrument (SIRS-A) was launched on NIMBUS-3 in 1969 (Wark and Hilleary, 1970). Successive experimental instruments on the NIMBUS series of polar orbiting satellites led to the development of the TIROS-N series of operational polar-orbiting satellites in 1978. These satellites introduced the TIROS Operational Vertical Sounder (TOVS, Smith et al. 1979), consisting of the High-resolution Infrared Radiation Sounder (HIRS), the Microwave Sounding Unit (MSU), and the Stratospheric Sounding Unit (SSU). This same series of instruments continues to fly today on the NOAA operational polar orbiting satellites. HIRS provides 17 km spatial resolution at nadir with 19 infrared sounding channels. The first sounding instrument in geostationary orbit was the GOES VISSR Atmospheric Sounder (VAS, Smith et al. 1981) launched in 1980. The current generation GOES-8 sounder (Menzel and Purdom, 1994) provides 8 km spatial resolution with 18 infrared sounding channels. An excellent review of the history of satellite temperature and moisture profiling is provided by Smith (1991).

2.3 Instrument Characteristics

MODIS is a scanning spectroradiometer with 36 spectral bands between 0.645 and 14.235 μm (King et al. 1992). Table 1 summarizes the MODIS technical specifications.

Table 1: MODIS Technical Specifications

Orbit:	705 km altitude, sun-synchronous, 10:30 a.m. descending node
Scan Rate:	20.3 rpm, cross track
Swath Dimensions:	2330 km (cross track) by 10 km (along track at nadir)
Quantization:	12 bits
Spatial Resolution:	250 m (bands 1-2), 500 m (bands 3-7), 1000 m (bands 8-36)

Table 2 shows the MODIS spectral bands that will be used in our MODIS algorithm . Note that in most cases the predicted (goal) noise is expected to be better than the specification. The data rate with 12 bit digitization and a 100% duty cycle is expected to be approximately 5.1×10^6 bits/sec (55 Gbytes/day).

Table 2: MODIS Spectral Band Specifications

Primary Atmospheric Application	Band	Bandwidth ¹	T _{typical} (K)	Radiance ² at T _{typical}	NEΔT (K) Specification	NEΔT (K) Predicted
Surface Temperature	20	3.660-3.840	300	0.45	0.05	0.05
	22	3.929-3.989	300	0.67	0.07	0.05
	23	4.020-4.080	300	0.79	0.07	0.05
Temperature profile	24	4.433-4.498	250	0.17	0.25	0.15
	25	4.482-4.549	275	0.59	0.25	0.10
Moisture profile	27	6.535-6.895	240	1.16	0.25	0.05
	28	7.175-7.475	250	2.18	0.25	0.05
	29	8.400-8.700	300	9.58	0.05	0.05
Ozone	30	9.580-9.880	250	3.69	0.25	0.05
Surface Temperature	31	10.780-11.280	300	9.55	0.05	0.05
	32	11.770-12.270	300	8.94	0.05	0.05
Temperature profile	33	13.185-13.485	260	4.52	0.25	0.15
	34	13.485-13.785	250	3.76	0.25	0.20
	35	13.785-14.085	240	3.11	0.25	0.25
	36	14.085-14.385	220	2.08	0.35	0.35

¹ μm at 50% response

² $\text{W m}^{-2} \text{sr}^{-1} \mu\text{m}^{-1}$

Figure 1 shows the spectral responses of the MODIS infrared bands in relation to an atmospheric emission spectrum computed by FASCOD3P for the US standard atmosphere.

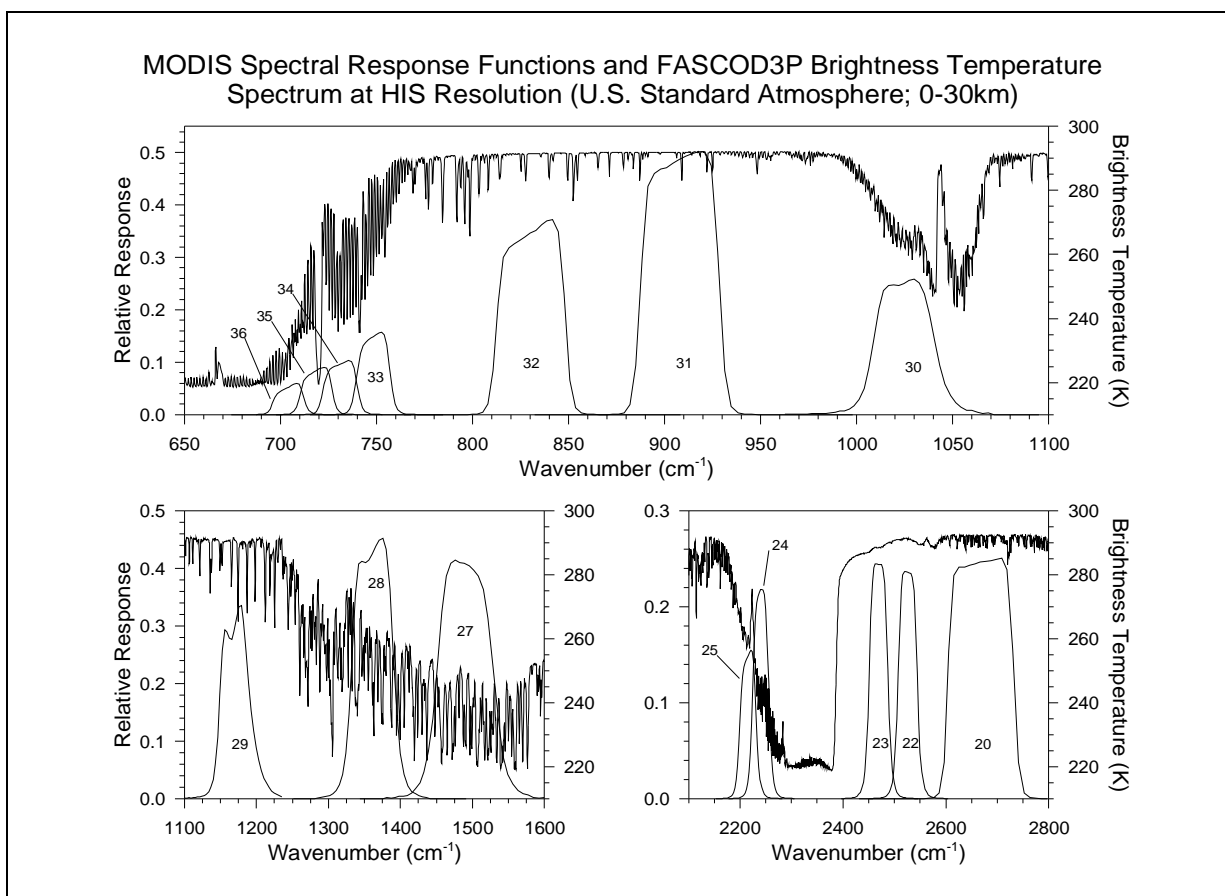


Figure 1: MODIS infrared spectral response. Nadir viewing emission spectrum of U.S. Standard Atmosphere from FASCOD3P.

3. Algorithm Description

In section we describe the theoretical basis and practical implementation of the atmospheric profile retrieval algorithm.

3.1 *Theoretical Background*

In order for atmospheric temperature to be inferred from measurements of thermal emission, the source of emission must be a relatively abundant gas of known and uniform distribution. Otherwise, the uncertainty in the abundance of the gas will make ambiguous the determination of temperature from the measurements. There are two gases in the earth-atmosphere which have uniform abundance for altitudes below about 100 km, and which also show emission bands in the spectral regions that are convenient for measurement. Carbon dioxide, a minor constituent with a relative volume abundance of 0.003, has infrared vibrational-rotational bands. In addition, oxygen, a major constituent with a relative volume abundance of 0.21, also satisfies the requirement of a uniform mixing ratio and has a microwave spin-rotational band.

There is no unique solution for the detailed vertical profile of temperature or an absorbing constituent because (a) the outgoing radiances arise from relatively deep layers of the atmosphere, (b) the radiances observed within various spectral channels come from overlapping layers of the atmosphere and are not vertically independent of each other, and (c) measurements of outgoing radiance possess errors. As a consequence, there are a large number of analytical approaches to the profile retrieval problem. The approaches differ both in the procedure for solving the set of spectrally independent radiative transfer equations (e.g., matrix inversion, numerical iteration) and in the type of ancillary data used to constrain the solution to insure a meteorologically meaningful result (e.g., the use of atmospheric covariance statistics as opposed to the use of an a priori estimate of the profile structure). There are some excellent papers in the literature which review the retrieval theory which has been developed over the past few decades (Fleming and Smith, 1971; Fritz et al., 1972; Rodgers, 1976; Twomey, 1977; and Houghton et al. 1984). The following sections present the mathematical basis for two of the procedures which have been utilized in the operational retrieval of atmospheric profiles from satellite measurements.

3.1.1a Statistical Regression Profile Retrieval

A computationally efficient method for determining temperature and moisture profiles from satellite sounding measurements uses previously determined statistical relationships between observed (or modeled) radiances and the corresponding atmospheric profiles. This method is often used to generate a first-guess for a physical retrieval algorithm, as is done in the International TOVS Processing Package (ITPP, Smith et al., 1993). The statistical regression algorithm for atmospheric temperature is described in detail in Smith et. al. (1970), and can be summarized as follows (the algorithm for moisture profiles is formulated similarly). In cloud-free skies, the radiation received at the top of the atmosphere at frequency ν is the sum of the radiance contributions from the Earth's surface and from all levels in the atmosphere,

$$R(\nu_j) = \sum_{i=1}^N B[\nu_j, T(p_i)] w(\nu_j, p_i) \quad (1)$$

where

$w(\nu_j, p_i) = \epsilon(\nu_j, p_i) \tau(\nu_j, 0 \rightarrow p_i)$ is the weighting function,

$B[\nu_j, T(p_i)]$ is the Planck radiance for pressure level i at temperature T ,

$\epsilon(\nu_j, p_i)$ is the spectral emissivity of the emitting medium at pressure level i ,

$\tau(\nu_j, 0 \rightarrow p_i)$ is the spectral transmittance of the atmosphere above pressure level i .

The problem is to determine the temperature (and moisture) at N levels in the atmosphere from M radiance observations. However because the weighting functions are broad and represent an average radiance contribution from a layer, the M radiance observations are interdependent, and hence there is no unique solution. Furthermore, the solution is unstable in that small errors in the radiance observations produce large errors in the temperature profile. For this reason, the solution is approximated in a linearized form. First (1) is re-written in terms of a deviation from an initial state,

$$R(\nu_j) - R_0(\nu_j) = \sum_{i=1}^N \{B[\nu_j, T(p_i)] - B[\nu_j, T_0(p_i)]\} w(\nu_j, p_i) + e(\nu_j) \quad (2)$$

where

$e(v_j)$ is the measurement error for the radiance observation.

In order to solve (2) for the temperature profile T it is necessary to linearize the Planck function dependence on frequency. This can be achieved since in the infrared region the Planck function is much more dependent on temperature than frequency. Thus the general inverse solution of (2) for the temperature profile can be written as

$$T(p_i) - T_0(p_i) = \sum_{j=1}^M A(v_j, p_i) [R(v_j) - R_0(v_j)] \quad (3)$$

or in matrix form

$$T = AR$$

where $A(v_j, p_i)$ is a linear operator. Referring back to (2), it can be seen that in theory A is simply the inverse of the weighting function matrix. However in practice the inverse is numerically unstable.

The statistical regression algorithm seeks a “best-fit” operator matrix A that is computed using least squares methods by utilizing a large sample of atmospheric temperature and moisture soundings, and collocated radiance observations. That is, we seek to minimize the error

$$\frac{\partial}{\partial A} |AR - T|^2 = 0$$

which is solved by the normal equations to yield

$$A = (R^T R)^{-1} R^T T \quad (5)$$

where

$(R^T R)$ is the covariance of the radiance observations,

$(R^T T)$ is the covariance of the radiance observations with the temperature profile.

The radiance observations may be from actual post-launch measurements, or computed pre-launch using a temperature and moisture sounding database, and weighting functions derived from knowledge of the sensor spectral responses. The coefficients of A may be updated as often as weekly, and different values for A are used depending on season and geographical location. In addition to the observed radiances, surface temperature and moisture

estimates may be used as predictors to improve the retrieval. The statistical regression algorithm has the advantage of computational speed, numerical stability, and simplicity. However it does not account for the physical properties of the Radiative Transfer Equation.

3.1.1b *Physical Profile Retrieval*

Direct physical solution of the Radiative Transfer Equation often involves several iterations between solving for the temperature and moisture profiles. They are interrelated but most solutions only solve for each one separately, assuming the other is known. Smith et al. (1985) have developed a simultaneous direct physical solution of both, and we follow this approach here. In order to solve for the temperature and moisture profiles simultaneously, a simplified form of the integral of the radiative transfer equation is considered,

$$R = B_0 + \int_0^{p_s} \tau dB,$$

which comes from integrating the atmospheric term by parts in the more familiar form of the RTE. R represents the radiance, τ the transmittance, and B the Planck radiance. Dependence on zenith angle, pressure, temperature, and frequency is assumed, but neglected in the notation for simplicity. The subscript s refers to the surface level and 0 refers to the top of the atmosphere. Then in perturbation form, where δ represents a perturbation with respect to an a priori condition

$$\delta R = \int_0^{p_s} (\partial \tau) dB + \int_0^{p_s} \tau d(\delta B).$$

Integrating the second term on right side of the equation by parts,

$$\int_0^{p_s} \tau d(\delta B) = \tau \delta B \Big|_0^{p_s} - \int_0^{p_s} \delta B d\tau = \tau_s \delta B_s - \int_0^{p_s} \delta B d\tau$$

yields

$$\delta R = \int_0^{p_s} (\partial \tau) dB + \tau_s \delta B_s - \int_0^{p_s} \delta B d\tau.$$

Now write the differentials with respect to temperature

$$\delta R = \delta T_b \frac{\partial B}{\partial T_b}, \quad \delta B = \delta T \frac{\partial B}{\partial T}$$

and with respect to pressure

$$dB = \frac{\partial B}{\partial T} \frac{\partial T}{\partial p} dp, \quad d\tau = \frac{\partial \tau}{\partial p} dp.$$

Substituting this in

$$\delta T_b = \int_0^{p_s} \delta \tau \frac{\partial T}{\partial p} \left[\frac{\partial B}{\partial T} / \frac{\partial B}{\partial T_b} \right] dp - \int_0^{p_s} \delta T \frac{\partial \tau}{\partial p} \left[\frac{\partial B}{\partial T} / \frac{\partial B}{\partial T_b} \right] dp + \delta T_s \left[\frac{\partial B_s}{\partial T_s} / \frac{\partial B}{\partial T_b} \right] \tau_s$$

where T_b is the brightness temperature. Finally, assume that the transmittance perturbation is dependent only on the uncertainty in the column of precipitable water density weighted path length u according to the relation

$$\delta \tau = \frac{\partial \tau}{\partial u} \delta u$$

Thus

$$\begin{aligned} \delta T_b &= \int_0^{p_s} \delta u \frac{\partial T}{\partial p} \frac{\partial \tau}{\partial u} \left[\frac{\partial B}{\partial T} / \frac{\partial B}{\partial T_b} \right] dp - \int_0^{p_s} \delta T \frac{\partial \tau}{\partial p} \left[\frac{\partial B}{\partial T} / \frac{\partial B}{\partial T_b} \right] dp + \delta T_s \left[\frac{\partial B_s}{\partial T_s} / \frac{\partial B}{\partial T_b} \right] \tau_s \\ &= f[\delta u, \delta T, \delta T_s] \end{aligned}$$

where f represents some function.

The perturbations are with respect to some a priori condition which may be estimated from climatology, regression, or more commonly from an analysis or forecast provided by a numerical model. In order to solve for δu , δT , and δT_s from a set spectrally independent radiance observations δT_b , the perturbation profiles are represented in terms of arbitrary basis functions $\phi(p)$; so

$$\begin{aligned} \delta T_s &= \alpha_0 \phi_0 \\ \delta u(p) &= \sum_{i=1}^Q \alpha_i \int_0^p q(p) \phi_i(p) dp \end{aligned}$$

where the water vapor mixing ratio is given by $q(p) = g \partial u / \partial p$ and $\delta q = g \sum \alpha_i q \phi$

$$\delta T(p) = - \sum_{i=Q+1}^L \alpha_i \phi_i(p).$$

Then for M spectral channel observations

$$\delta T_{bj} = \sum_{i=0}^L \alpha_i \psi_{ij} \quad \text{where } j = 1, \dots, M$$

and

$$\begin{aligned}\Psi_{0j} &= \left[\frac{\partial B_j}{\partial T_s} / \frac{\partial B_j}{\partial T_{bj}} \right] \tau_{sj}, \\ \Psi_{ij} &= \int_0^{p_s} \left[\int_0^p q \phi_i dp \right] \left[\frac{\partial T}{\partial p} \frac{\partial \tau_j}{\partial u} \right] \left[\frac{\partial B_j}{\partial T} / \frac{\partial B_j}{\partial T_{bj}} \right] dp, \quad i = 1, \dots, Q \\ \Psi_{ij} &= \int_0^{p_s} \phi_i \frac{\partial \tau_j}{\partial p} \left[\frac{\partial B_j}{\partial T} / \frac{\partial B_j}{\partial T_{bj}} \right] dp, \quad i = Q+1, \dots, L\end{aligned}$$

or in matrix form

$$t_b = \Psi \alpha.$$

A least squares solution suggests that

$$\alpha = (\Psi^t \Psi)^{-1} \Psi^t t_b \approx (\Psi^t \Psi + \gamma I)^{-1} \Psi^t t_b$$

where the Lagrangian multiplier is incorporated to stabilize the matrix inverse.

There are many reasonable choices for the pressure basis functions $\phi(p)$. For example empirical orthogonal functions (eigenvectors of the water vapor and temperature profile covariance matrices) can be used in order to include statistical information in the solution. Also the profile weighting functions of the radiative transfer equation can be used, as can Gaussian functions that peak in different layers of the atmosphere. We intend to use the transmittance profile weighting functions as the basis functions in the MODIS temperature and moisture profile retrieval algorithm. Examples of these functions are shown in Figure 2.

Ancillary information, such as surface observations, are readily incorporated into the profile solutions as additional equations (M+2 equations to solve L unknowns).

$$\begin{aligned}q_0 - q(p_s) &= g \sum_{i=1}^Q \alpha_i q(p_s) \phi_i(p_s) \\ T_0 - T(p_s) &= - \sum_{i=Q+1}^L \alpha_i \phi_i(p_s)\end{aligned}$$

In summary we have the following characteristics (a) the RTE is in perturbation form, (b) δT and δU are expressed as linear expansions of basis functions (empirical orthogonal functions or weighting functions), (c) ancillary observations are used as extra equations, (d) a

least squares solution is sought, and (e) a simultaneous temperature and moisture profile solution produces improved moisture determinations.

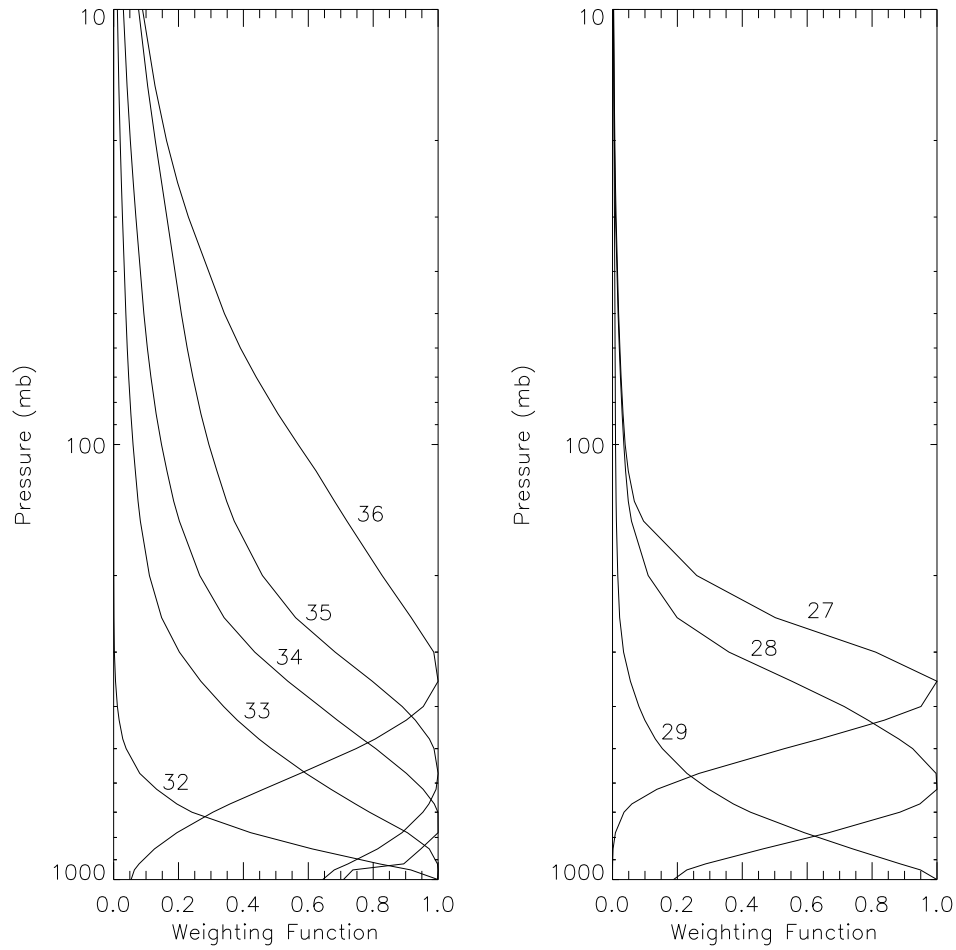


Figure 2: MODIS temperature (left) and moisture (right) normalized retrieval weighting functions ($\partial\tau/\partial\ln p$) for the U.S. Standard Atmosphere at nadir view from FASCOD3P.

The simultaneous solution addresses the interdependence of water vapor radiance upon temperature and carbon dioxide channel radiance upon water vapor concentration. The dependence of the radiance observations on the surface emissions is accounted for by the inclusion of surface temperature as an unknown. Our experience has shown that a single matrix solution is more computationally efficient than an iterative calculation.

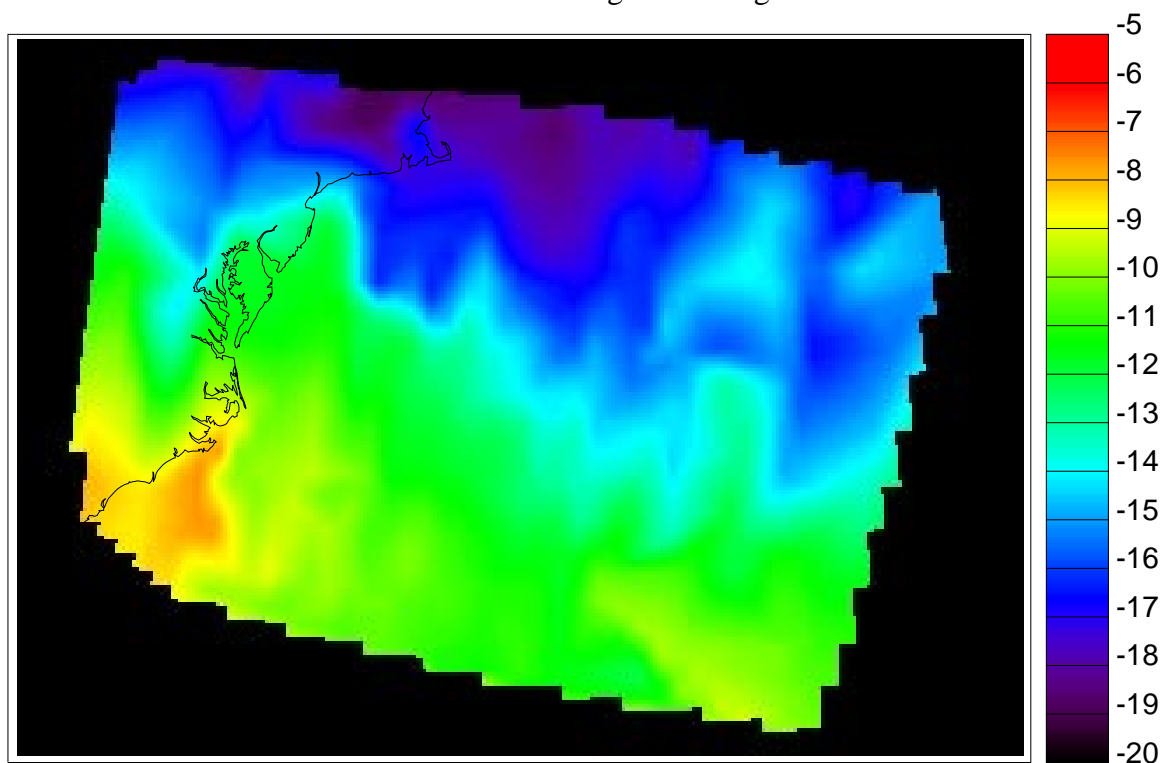
Sullivan et al. (1993) present results from a physical HIRS retrieval algorithm, and show global RMS differences between HIRS retrieved and collocated radiosonde measured temperature profiles of ≈ 1.9 C between 700 and 300 hPa. At the tropopause and near the Earth surface these values increase by ≈ 0.5 -1.0 C. In cloudy conditions, another degree of separation between HIRS profile retrieval and radiosonde observations is found. Differences should not be interpreted literally as retrieval error; space and time discrepancies between the two types of observations contribute significantly as does atmospheric variability.

In the absence of any spectral bands sensitive to the stratosphere (bands with center wavelengths from 14.5 to 15.0 μm), the profile retrievals from the MODIS will rely on the global numerical forecast models (such as the NCEP Global Data Assimilation System, GDAS) for this information. Since the stratosphere is largely stable and slowly varying, the model should be very representative of the stratospheric conditions and the accuracy of the MODIS temperature and moisture profiles should not be significantly affected. Because MODIS has significantly higher spatial resolution (1 km MODIS versus 17 km HIRS at nadir) and maintains good signal to noise, clear sky radiance determinations will be more accurate and the retrieval coverage and accuracy is expected to be enhanced with respect to that reported in the preceding paragraph for HIRS (how much better remains to be seen from actual data). Figure 3 shows HIRS physical and statistical retrievals of the 500 hPa temperature field. Good agreement is noted.

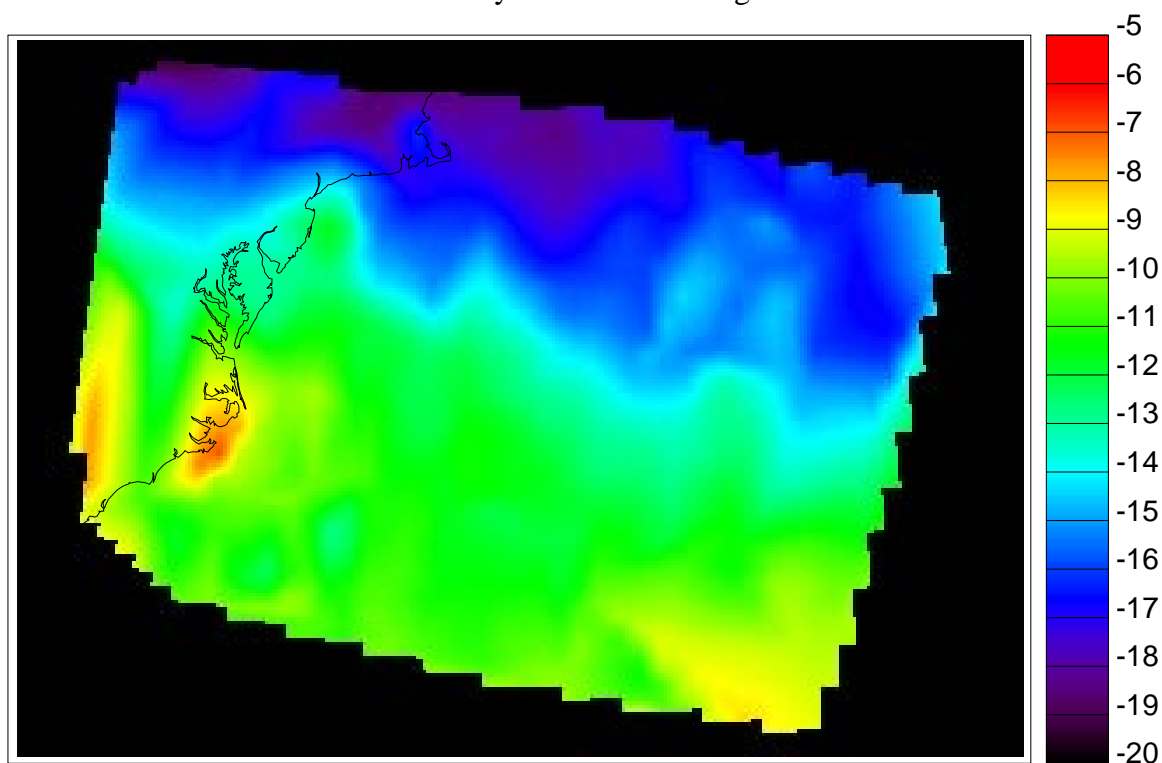
The retrieval of atmospheric profiles over land surfaces is usually not hindered by surface emissivity effects. There are several reasons for this. Foremost is the fact that the infrared window radiance provides a very good estimate of the effective radiating temperature, T_{eff} , for the surface (where $B(T_{eff}) = \epsilon_{sfc} B(T_{sfc})$). This can be used to infer the surface contribution of the radiative transfer equation for the infrared sounding bands since the surface emissivity remains roughly the same in this part of the infrared spectrum (the earth surface behaves like a gray body for the infrared sounding bands). Additionally, much of the retrieval skill between 300 and 850 hPa comes from infrared spectral bands that do not see the earth surface or receive only a fraction of their radiation from the surface.

Figure 3: NOAA-12 95/05/15 1210-1214 UTC 500 hPa temperature (degrees C).

ITPP 5.0 Statistical Regression Algorithm



ITPP 5.0 Physical Retrieval Algorithm



3.1.2 Total Column Ozone

Ozone is an important atmospheric constituent found in the atmosphere between 10 and 50 km above the earth's surface. Because it absorbs ultraviolet rays from the sun, ozone protects man from the harmful effects of ultraviolet radiation. Also, ozone is a prime source of thermal energy in the low stratosphere and has been shown to be a useful tracer for stratospheric circulation. Prabhakara et al. (1970) have exploited remote sensing of the total ozone using satellite infrared emission measurements and their studies reveal a strong correlation between the meridional gradient of total ozone and the wind velocity at tropopause levels. Shapiro et al. (1982) have indicated a possibility to predict the position and intensity of jet streams using total ozone measured by satellite.

Ma et al. (1984) described a method for obtaining total ozone with high spatial resolution from the TIROS-N/NOAA series of satellites. The ozone concentration is mapped with the 9.6 μm ozone radiance observations obtained by HIRS. The influence of clouds must be screened out to produce reliable ozone determinations.

Ozone concentration is related to radiance to space through the transmittance $\tau(p)$. The total column ozone can be estimated from 9.6 μm observations of a scene. The 9.6 μm channel radiance measurements are comprised of contributions from stratospheric ozone amount and temperature as well as surface temperature and boundary layer water vapor. Assuming that the temperature profile and the surface temperature is well known for a given FOV, then the perturbation form of the radiative transfer equation reduces to

$$\delta T_{oz} = \int_0^{p_s} \delta \tau \frac{\partial T}{\partial p} \left[\frac{\partial B}{\partial T} / \frac{\partial B}{\partial T_{oz}} \right] dp$$

where T_{oz} is the 9.6 μm brightness temperature. Finally, assume that the transmittance perturbation is dependent only on the uncertainty in the column of ozone density weighted path length v according to the relation

$$\delta \tau = \frac{\delta T}{\partial v} \delta v$$

Thus

$$\begin{aligned}\delta T_{oz} &= \int_0^{p_s} \delta v \frac{\partial T}{\partial p} \frac{\partial \tau}{\partial v} \left[\frac{\partial B}{\partial T} / \frac{\partial B}{\partial T_{oz}} \right] dp \\ &= f[\delta v]\end{aligned}$$

where f represents some function.

As in the profile retrieval, the perturbations are with respect to some a priori condition which may be estimated from climatology, regression, or more commonly from an analysis or forecast provided by a numerical model. In order to solve for δv from the 9.6 μm radiance observations δT_{oz} , the perturbation profile is represented in terms of the 9.6 μm weighting function (used as the basis function $\phi(p)$); so

$$\delta v = \alpha \phi$$

where α is computed from the initial guess.

The profile shape and the vertical position of the peak ozone mixing ratio corresponding to the ozone guess profile is crucial to obtaining a satisfactory retrieval since only one ozone channel radiance in the 9.6 μm band is used. This is because the true ozone profile is assumed to have the same shape as the first guess. Therefore, to make the ozone guess profile sufficiently accurate in both shape and position of the ozone peak mixing ratio, adjustments to the vertical position and amplitude of the guess peak mixing ratio are made based on the difference between the observed brightness temperature and the calculated brightness temperature using the ozone guess profile. Specifically the vertical position is adjusted by

$$Dp = a + b(T_{oz}^{cal} - T_{oz}^{obs})$$

where a and b are dependent on latitude and are obtained from linear regression in an independent set of conventional sounding data.

An alternate approach for estimating total atmospheric column ozone follows the NOAA operational HIRS algorithm. Total ozone is separated into upper and lower stratospheric contributions. Warm ozone in the upper stratosphere would be estimated directly from the model first guess; cold ozone in the lower stratosphere is estimated directly from its effect on the 9.6 μm channel radiance. Determination of lower stratospheric ozone requires an estimate of foreground temperature T_f and background temperature T_b . T_f is estimated from the model first guess 50 mb temperature. T_b is estimated from the infrared window brightness

temperature in the absence of any ozone. The effects of upper stratospheric ozone are removed from the 9.6 μm radiance value by the following extrapolation

$$R'_{oz} = [R_{oz} - A_u R(30\text{mb})] / [1 - A_u]$$

where from the model first guess we calculate

$$\begin{aligned} A_u &= 0.18 \sqrt{E_{su}}, \\ E_{su} &= E_q(\text{lat}) + S_w, \\ E_q &= 0.9 + 1.1 \cos(\text{lat}), \\ S_w &= D_T [1 + D_T (2 + D_T)] [270 + \text{lat}] / 9000, \\ D_T &= L_R W_A / 40, \\ L_R &= T(60\text{mb}) - T(100\text{mb}) - 1 = \text{tropospheric lapse rate}, \\ W_A &= 2T(60\text{mb}) - T(30\text{mb}) - 205 = \text{lower stratospheric temperature anomaly}. \end{aligned}$$

Then

$$R'_{oz} = \tau_{ls} R_b + (1 - \tau_{ls}) R_f$$

where τ_{ls} is the transmittance through the lower stratosphere, R_b is the radiance from the background, and R_f is the radiance from the foreground. Solving for τ_{ls} yields the amount of total ozone by inverting Beer's law.

It is not known yet which algorithm will perform better with MODIS data, where the stratospheric temperatures are not measured. Both are currently under investigation. Simulations and real data retrievals indicate that the total ozone concentration can be retrieved with an accuracy better than 10%.

3.1.3 Total column precipitable water vapor

Determination of the total column precipitable water vapor is most directly done by integrating the moisture profile through the atmospheric column. However several other simpler approaches are also viable. They are briefly described below.

The split window method can be used to specify total water vapor concentration from clear sky 11 μm and 12 μm brightness temperature measurements. The water vapor is evaluated by observing the area of interest in both infrared window channels. In the atmospheric window regions the absorption is weak so that

$$\tau_w = e^{-K_w u} \approx 1 - K_w u$$

where w denotes the window channel wavelength. Thus

$$d\tau_w = -K_w du$$

What little absorption exists is due to water vapor, therefore, u is a measure of precipitable water vapor. The measured radiance in the window region can be written from the RTE

$$R_w = B_{sw}(1 - K_w u_s) + K_w \int_0^{u_s} B_w du$$

where s denotes surface, and u_s represents the total atmospheric column absorption path length due to water vapor. Defining an atmospheric mean Planck radiance

$$\bar{B}_w = \int_0^{u_s} B_w du \bigg/ \int_0^{u_s} du$$

then

$$R_w = B_{sw}(1 - K_w u_s) + K_w u_s \bar{B}_w$$

Since B_{sw} is close to both R_w and B_w , first order Taylor expansion about the surface temperature T_s allows us to linearize the RTE with respect to temperature, so

$$T_{bw} = T_s(1 - K_w u_s) + K_w u_s \bar{T}_w$$

where \bar{T}_w is the mean atmospheric temperature corresponding to B_w . This implies that

$$u_s = [T_{bw} - T_s] / [K_w(\bar{T}_w - T_s)]$$

Obviously, the accuracy of the determination of the total water vapor concentration depends upon the contrast between the surface temperature and the effective temperature of the atmosphere. In an isothermal situation, the total precipitable water vapor concentration is indeterminate. For two window channel wavelengths (11 and 12 μm) the split window approximation allows us to write

$$T_s = [K_{w2} T_{bw1} - K_{w1} T_{bw2}] / [K_{w2} - K_{w1}]$$

and if we express T_w as proportional to T_s

$$\bar{T}_w = a_w T_s$$

then a solution for u_s follows:

$$\begin{aligned}
u_s &= \frac{T_{bw2} - T_{bw1}}{(a_{w1} - 1)(K_{w2}T_{bw1} - K_{w1}T_{bw2})} \\
&= \frac{T_{bw2} - T_{bw1}}{b_1T_{bw1} - b_2T_{bw2}}
\end{aligned}$$

The coefficients b_1 and b_2 can be evaluated in a linear regression analysis from prescribed temperature and water vapor profile conditions coincident with in situ observations of u_s . The weakness of the method is due to the time and spatial variability of a_w and the insensitivity of a stable lower atmospheric state when $T_{bw1} \sim T_{bw2}$ to the total precipitable water vapor concentration.

Another approach lies in the Split Window Variance Ratio, which starts from atmospheric windows with minimal moisture absorption

$$R_w = B_{sw}(1 - K_w u_s) + K_w u_s \bar{B}_w$$

Consider neighboring fields of view and assume that the air temperature is invariant, then the gradients can be written

$$DR_w = DB_{sw}(1 - K_w u_s)$$

where D indicates the differences due to different surface temperatures in the two FOVs. Convert to brightness temperatures with a Taylor expansion with respect to one of the surface temperatures, so that

$$\begin{aligned}
[R_w(FOV1) - R_w(FOV2)] &= [B_{sw}(FOV1) - B_{sw}(FOV2)][1 - K_w u_s] \\
[T_w(FOV1) - T_w(FOV2)] &= [T_s(FOV1) - T_s(FOV2)][1 - K_w u_s]
\end{aligned}$$

Using the split windows we can arrive at an estimate for u_s in the following way. Write the ratio

$$\begin{aligned}
\frac{1 - K_{w1}u_s}{1 - K_{w2}u_s} &= \frac{dR_{w1}dB_{sw2}}{dR_{w2}dB_{sw1}} \\
&= \frac{[R_{w1}(FOV1) - R_{w1}(FOV2)][B_{sw2}(FOV1) - B_{sw2}(FOV2)]}{[R_{w2}(FOV1) - R_{w2}(FOV2)][B_{sw1}(FOV1) - B_{sw1}(FOV2)]} \\
&= \frac{[T_{w1}(FOV1) - T_{w1}(FOV2)][T_s(FOV1) - T_s(FOV2)]}{[T_{w2}(FOV1) - T_{w2}(FOV2)][T_s(FOV1) - T_s(FOV2)]} \\
&= \frac{[T_{w1}(FOV1) - T_{w1}(FOV2)]}{[T_{w2}(FOV1) - T_{w2}(FOV2)]}
\end{aligned}$$

since the surface temperature cancels out. Therefore

$$\frac{1 - K_{w1}u_s}{1 - K_{w2}u_s} = \frac{DT_{w1}}{DT_{w2}}$$

or

$$u_s = (1 - D_{12}) / (K_{w1} - K_{w2}D_{12})$$

where D_{12} represents the ratio of the deviations of the split window brightness temperatures. The deviation is often determined from the square root of the variance.

The assumption in this technique is that the difference in the brightness temperatures from one FOV to the next is due only to the different surface temperatures. It is best applied to an instrument with relatively good spatial resolution, so that sufficient samples can be found in an area with small atmospheric variations and measurable surface variations in order to determine the variance of the brightness temperatures accurately. The technique was suggested by the work of Chesters et al (1983) and Kleespies and McMillin (1984); Jedlovec (1987) successfully applied it to aircraft data with 50 m spatial resolution to depict mesoscale moisture variations preceding thunderstorm development.

Total precipitable water vapor can be retrieved with an accuracy of 10% with respect to determination from radiosondes. Again not all of this difference should be construed as error but as a reflection on the differences of observation (point measurement versus area average) and differences of location in space and time.

3.1.4 Atmospheric Stability

One measure of the thermodynamic stability of the atmosphere is the total-totals index, defined by

$$TT = T_{850} + TD_{850} - 2T_{500}$$

where T_{850} and T_{500} are the temperatures at the 850 mb and 500 mb levels, respectively, and TD_{850} is the 850-mb level dew point. TT is traditionally estimated from radiosonde point values. For a warm moist atmosphere underlying cold mid-tropospheric air, TT is high (e.g., 50-60 K) and intense convection can be expected. There are two limitations of radiosonde derived TT : (a) the spacing of the data is too large to isolate local regions of probable convection and (b) the data are not timely since they are available only twice per day.

If we define the dew point depression at 850 mb, $D_{850} = T_{850} - TD_{850}$, then

$$TT = 2(T_{850} - T_{500}) - D_{850}$$

Although point values of temperature and dew point cannot be observed by satellite, the layer quantities observed can be used to estimate the temperature lapse rate of the lower troposphere ($T_{850} - T_{500}$) and the low level relative moisture concentration D_{850} . Assuming a constant lapse rate of temperature between the 850 and 200 mb pressure levels and also assuming that the dew point depression is proportional to the logarithm of relative humidity, it can be shown from the hydrostatic equation that

$$TT = 0.1489DZ_{850-500} - 0.0546DZ_{850-200} + 16.03\ln(RH)$$

where DZ is the geopotential thickness in meters and RH is the lower tropospheric relative humidity, both estimated from the MODIS radiance measurements as explained earlier.

Smith and Zhou (1982) reported several case studies using this approach. They found general agreement in gradients in space and time, with the satellite data providing much more spatial detail than the sparse radiosonde observations.

Another estimate of atmospheric stability is the lifted index, which can be derived from the MODIS determined temperature and moisture profile. The lifted index is the difference of the measured 500 mb temperature and the temperature calculated by lifting a surface parcel dry adiabatically to its local condensation level and then moist adiabatically to 500 mb. As this value goes negative it indicates increased atmospheric instability.

3.1.5 *Estimate of Errors*

A complete error analysis including the effects of instrument calibration and noise as well as ancillary input data errors remains to be completed. The past performance of these algorithms with HIRS data is documented as temperature profiles errors at about 1.9 C, dewpoint temperature profile errors at about 4 C, total column ozone at about 10%, total column water vapor at about 10%, and gradients in atmospheric stability within 0.5 C.

The profile and total atmospheric columns algorithms are based on HIRS experience. One significant difference between MODIS and HIRS is the absence of any stratospheric channels on MODIS (15.0, 14.7, and 14.5 μm). This will primarily affect the accuracy of the total ozone concentration estimates. The assumption for the MODIS algorithms presented here is that the slowly varying stratospheric temperatures are estimated very well by the forecast

model. The higher spatial resolution of the MODIS compared to the HIRS will make clear sky radiance estimates more accurate and hence the RMS errors of the profile retrievals can be expected to improve (possibly by 0.5 C but exactly how much remains to be seen from actual data).

3.2 *Practical Considerations*

The MODIS infrared CO₂ and H₂O channels will be used to investigate the clear sky atmosphere at 5×5 pixel resolution and to generate a global census of atmospheric stability and total precipitable water and total ozone at 5×5 pixel resolution.

3.2.1 *Radiance Biases and Numerical Considerations*

The MODIS measured radiances will have biases with respect to the forward calculated radiances using model estimates of the temperature and moisture profile for a given field of view. There are several possible causes for this bias: these include calibration errors, spectral response uncertainty, undetected cloud in the FOV, and model uncertainty. The physical retrieval method uses measured and calculated radiances (using the first guess) and thus requires that this bias be minimized. Techniques developed at the European Centre for Medium range Weather Forecast to characterize the HIRS radiance bias with respect to the ECMWF model (Eyre, 1992) will be employed in the MODIS atmospheric profile algorithm. The transmittance model will be developed using the methods outlined by Eyre and Woolf (1988), using FASCOD3P as the reference source.

3.2.2 *Data Processing Considerations*

Processing will be accomplished globally at 5×5 pixel resolution in regions where a sufficient number of clear FOVs are available (the threshold number of clear FOVs will be determined when instrument noise equivalent radiances are estimated in vacuum test). Clear FOVs will be averaged to reduce instrument single sample noise.

An estimate of the processing requirements for this algorithm follows. Timing tests were conducted on a Silicon Graphics Power Indigo² (R8000/75 Mhz). The Version 1 MODIS atmospheric profiles code (statistical regression only) was run on simulated cloud-free MODIS Level 1B radiance data supplied by the MODIS Science Data Support Team. The input dataset contained 100 MODIS scans, which translates to 1000 along track 1 kilometer

pixels. Processing was done on 5×5 blocks of pixels, and input data included the Level 1B radiances, corresponding geolocation data, simulated cloud mask data, and ancillary data (surface temperature and water vapor mixing ratio). The timing shown below reflects all phases of the processing, including opening and reading input data files, computing retrieval parameters, and writing the output data file. Timing was measured using the Unix ‘timex’ command. Results are shown in Table 3.

Table 3: Timing test results for MODIS atmospheric profiles code (statistical regression)

Real	484.4 sec
User	134.2 sec
System	301.7 sec

3.2.3 Validation

Validation of the MODIS atmospheric profiles and derived parameters will be approached in several ways. Well-calibrated radiances are essential for the development of accurate algorithms. We plan to verify the MODIS infrared radiances by using collocated data from two sensors onboard a NASA ER-2 high altitude aircraft. The MAS is a fifty channel visible, near-infrared, and thermal infrared scanning spectrometer with 50 m spatial resolution at nadir (King et al. 1996), and the HIS is a nadir-viewing Michelson interferometer with 0.5 cm^{-1} spectral resolution from 4 to $15 \text{ }\mu\text{m}$ (Revercomb et al. 1988) and 2 km spatial resolution at nadir. The calibration of the HIS is such that it serves as a reference for line-by-line radiative transfer models. The MAS infrared channels are calibrated through two onboard blackbody sources that are viewed once every scan, taking into account the spectral emissivity of the blackbodies. Our first coordinated validation campaign would occur within the first year after MODIS launch, and would be a land-based field campaign with the ER-2 over the ARM CART site in Oklahoma. Data to be collected would include simultaneous ground-based CLASS-sonde temperature and moisture profiles, AERI (a ground-based Michelson interferometer) uplooking radiance spectra, tower measurements of temperature and moisture at various elevations, microwave moisture measurements, lidar and radar cloud observations,

and whole sky camera images. Two field campaigns at the CART site are planned (Aug.-Sep. 1998 and Apr.-May 1999).

MODIS retrievals from the calibrated radiances will be compared to those determined from in situ radiosonde measurements, the NOAA HIRS operational retrievals, the GOES sounder operational retrievals, NCEP analysis of all available data, and retrievals from the Atmospheric Infrared Sounder (AIRS/AMSU/MHS) on the EOS PM-1 platform. Total ozone will be compared to Total Ozone Mapping Spectrometer (TOMS) measurements as well as the operational NOAA ozone estimates from HIRS. A field campaign utilizing the profiler network in the US midwest with CLASS sondes and ground based (Atmospheric Emitted Radiances Interferometer, AERI) and airborne ER-2 (High resolution Interferometer Sounder, HIS) measurements and with airborne MODIS Airborne Simulator measurements will also be initiated in the first year after launch to further validate the MODIS retrievals. Precipitable water vapor measurements will be compared to (i) radiosonde measurements over the continents, (ii) model output obtained as part of the EOS data assimilation interdisciplinary science team (Dr. Richard Rood), and (iii) periodic differential absorption lidar measurements from the ER-2 aircraft (LASE; Dr. Ed Browell).

3.2.4 Quality Control

Quality control will be accomplished by manual and automatic inspection of the data and comparison to other sources of information. Automatic tests will check for physically realistic output values of temperature and moisture. Regional and global mean temperatures at 300, 500, and 700 mb will be monitored for weekly consistency; similarly dew point temperatures at 700 mb will be monitored. Global and regional precipitable water will also be tracked for spurious trends. Ozone in the polar regions will be averaged regionally and monitored for weekly consistency. Acceptable variations from week to week will be determined from the actual data.

3.2.5 Exception Handling

The algorithm will check the validity of input radiances using metadata attached to the data itself, and validity tests developed post-launch. If the required input radiance data is bad, suspect, or not available, then the algorithm will record the output products as missing for that 5×5 pixel area.

3.2.6 Data Dependencies

The profile retrieval algorithm requires calibrated, navigated, coregistered 1 km FOV radiances from channels 20 (3.75 μm shortwave window), 22-25 (3.96 to 4.52 μm shortwave CO₂ absorption band), 27-29 (6.72 to 8.55 μm for moisture information), 30 (9.73 μm for ozone), 31-32 (11.03 and 12.02 split window), and 33-36 (13.34, 13.64, 13.94, and 14.24 μm CO₂ absorption band channels). The MODIS Cloud Mask will be also used for cloud screening, and for surface type determination (land or sea). The MODIS viewing angle for a given FOV must be known. The NCEP global model estimates of surface temperature and pressure as well as profiles of temperature and moisture will be initially used in the calculation; as the AIRS/AMSU profiles become available, they will also be used.

3.2.7 Output Product Description

Four products will be generated as part of the MODIS atmospheric profile retrieval algorithm. Product MOD30 (Atmospheric Profiles) will contain retrieved vertical profiles of temperature and moisture. Products MOD07 (Total Ozone Burden), MOD38 (Atmospheric Water Vapor), and MOD08 (Atmospheric Stability) are generated as part of the processing for MOD30, and as such are considered part of the atmospheric profiles product. The parameters generated as for these four products are shown in Table 4.

Table 4: Parameters included in products MOD30, MOD07, MOD38, MOD08Resolution: 5×5 pixel, Temporal sampling: Day and Night, Restrictions: Clear Sky only

Parameter Name	Expected Range, Units	Storage Format	Bytes
Time of observation (past 0 UTC)	0:86400000, msec	Long Integer	4
Latitude	-90:90, degrees	Float	4
Longitude	-180:180, degrees	Float	4
Scanline number	TBD, no units	Long Integer	4
Pixel number	1:1354, no units	Short Integer	2
Satellite zenith angle	0:55, degrees	Float	4
Solar zenith angle	0:90, degrees	Float	4
Land/sea flag	0:1, no units	Byte	1
IR channel brightness temperatures bands 20, 22-25, 27-36 (15 total)	150:350, K	Short Integer	30
Estimated surface temperature	150:350, K	Short Integer	2
Estimated surface pressure	800:1200, mb	Short Integer	2
Tropopause height estimate	0:15000, m	Short Integer	2
Guess temperature at 20 levels	150:350, K	Short Integer	40
Guess dewpoint at 20 levels	150:350, K	Short Integer	40
Retrieved temperature at 20 levels	150:350, K	Short Integer	40
Retrieved dewpoint at 20 levels	150:350, K	Short Integer	40
Total Ozone Burden	0:500, Dobson units	Short Integer	2
Atmospheric Water Vapor	0:1000, mm	Short Integer	2
Stability Indices (3 total)	TBD, K	Short Integer	6

4. Assumptions

The data are assumed to be calibrated (within the instrument noise), navigated (within one FOV), and coregistered (within two tenths of a FOV). The accuracy of the retrievals will depend on the on-orbit NE Δ T values in the infrared channels, estimates of which were shown in Table 2. It is assumed that high-quality global forecast model (e.g. NCEP, ECMWF, or GSFC/DAO) output or analysis fields will present for the derivation of first guess temperature and moisture profiles, since the retrieval algorithm essentially adjusts the guess just enough to fit the measured radiances.

5. References

- Chesters, D., Uccellini, L. W. and W. D. Robinson, 1983: Low-level water vapor fields from the VISSR Atmospheric Sounder (VAS) “split window” channels. *J. Clim. Appl. Met.*, **22**, 725-743.
- Eyre, J. R., and H. M. Woolf, 1988: Transmittance of atmospheric gases in the microwave region: a fast model. *Appl. Opt.*, **25**, 3244-3249.
- _____, 1992: A bias correction scheme for simulated TOVS brightness temperatures. *ECMWF Technical Memorandum 186*. 28 pp.
- Fleming, H. E. and W. L. Smith, 1971: Inversion techniques for remote sensing of atmospheric temperature profiles. *Reprint from Fifth Symposium on Temperature*. Instrument Society of America, 400 Stanwix Street, Pittsburgh, Pennsylvania, 2239-2250.
- Fritz, S., D. Q. Wark, H. E. Fleming, W. L. Smith, H. Jacobowitz, D. T. Hilleary, and J. C. Alishouse, 1972: Temperature sounding from satellites. *NOAA Technical Report NESS 59*. U.S. Department of Commerce, National Oceanic and Atmospheric Administration, National Environmental Satellite Service, Washington, D.C., 49 pp.
- Hayden, C. M., 1988: GOES-VAS simultaneous temperature-moisture retrieval algorithm. *J. Appl. Meteor.*, **27**, 705-733.
- Houghton, J. T., Taylor, F. W., and C. D. Rodgers, 1984: Remote Sounding of Atmospheres. Cambridge University Press, Cambridge UK, 343 pp.
- Jedlovec, G. J., 1987: Determination of atmospheric moisture structure from high resolution MAMS radiance data. Ph. D. Thesis, University of Wisconsin - Madison.
- Kaplan, L. D., 1959: Inference of atmospheric structure from remote radiation measurements. *Journal of the Optical Society of America*, **49**, 1004.
- King, J. I. F., 1956: The radiative heat transfer of planet earth. *Scientific Use of Earth Satellites*, University of Michigan Press, Ann Arbor, Michigan, 133-136.
- King, M.D., Kaufman, Y. J., Menzel, W. P. and D. Tanré, 1992: Remote sensing of cloud, aerosol, and water vapor properties from the Moderate Resolution Imaging Spectrometer (MODIS). *IEEE Trans. Geosci. Remote Sens.*, **30**, 2-27.
- _____, Menzel, W. P., Grant, P. S., Myers, J. S., Arnold, G. T., Platnick, S. E., Gumley, L. E., Tsay, S. C., Moeller, C. C., Fitzgerald, M., Brown, K. S. and F. G. Osterwisch, 1996:

- Airborne scanning spectrometer for remote sensing of cloud, aerosol, water vapor and surface properties. *J. Atmos. Oceanic Technol.*, **13**, 777–794.
- Kleespies, T. J. and L. M. McMillin, 1984: Physical retrieval of precipitable water using the split window technique. Preprints Conf. on Satellite Meteorology/Remote Sensing and Applications, AMS, Boston, 55-57.
- Ma, X. L., Smith, W. L. and H. M. Woolf, 1984: Total ozone from NOAA satellites-a physical model for obtaining observations with high spatial resolution. *J. Climate Appl. Meteor.*, **23**, 1309-1314.
- Menzel, W. P., and J. F. W. Purdom, 1994: Introducing GOES-I: The first of a new generation of geostationary operational environmental satellites. *Bull. Amer. Meteor. Soc.*, **75**, 757-781.
- Prabhakara, C., Conrath, B. J. and R. A. Hanel, 1970: Remote sensing of atmospheric ozone using the 9.6 μm band. *J. Atmos. Sci.*, **26**, 689-697.
- Revercomb, H. E., Buijs, H. , Howell, H. B., LaPorte, D. D. , Smith, W. L. and L. A. Sromovsky, 1988: Radiometric Calibration of IR Fourier Transform Spectrometers: Solution to a Problem with the High Resolution Interferometer Sounder. *Applied Optics*, **27**, 3210-3218.
- Rodgers, C. D., 1976: Retrieval of atmospheric temperature and composition from remote measurements of thermal radiation. *Rev. Geophys. Space Phys.*, **14**, 609-624.
- Shapiro, M. A., Krueger, A. J. and P. J. Kennedy, 1982: Nowcasting the position and intensity of jet streams using a satellite borne total ozone mapping spectrometer. *Nowcasting*, K. A. Browning (ed.), Academic Press, Inc., (London) Ltd., 137-145.
- Smith, W. L., Woolf, H. M., and W. J. Jacob, 1970: A regression method for obtaining real-time temperature and geopotential height profiles from satellite spectrometer measurements and its application to Nimbus 3 “SIRS” observations. *Mon. Wea. Rev.*, **8**, 582-603.
- _____, Woolf, H. M., Hayden, C. M., Wark, D. Q. and L. M. McMillin, 1979: The TIROS-N operational vertical sounder. *Bull. Amer. Meteor. Soc.*, **60**, 1177-1187.

- _____, Suomi, V. E., Menzel, W. P., Woolf, H. M., Sromovsky, L. A., Revercomb, H. E., Hayden, C. M., Erickson, D. N. and F. R. Mosher, 1981: First sounding results from VAS-D. *Bull. Amer. Meteor. Soc.*, **62**, 232-236.
- _____, and F. X. Zhou, 1982: Rapid extraction of layer relative humidity, geopotential thickness, and atmospheric stability from satellite sounding radiometer data. *Appl. Opt.*, **21**, 924-928.
- _____, Woolf, H. M. and A. J. Schriener, 1985: Simultaneous retrieval of surface and atmospheric parameters: a physical and analytically direct approach. *Advances in Remote Sensing*, A. Deepak, H. E. Fleming, and M. T. Chahine (Eds.), ISBN 0-937194-07-7, 221-232.
- _____, and H. M. Woolf, 1988: A Linear Simultaneous Solution for Temperature and Absorbing Constituent Profiles from Radiance Spectra. Technical Proceedings of the Fourth International TOVS Study Conference held in Igls, Austria 16 to 22 March 1988, W. P. Menzel Ed., 330-347.
- _____, 1991: Atmospheric soundings from satellites - false expectation or the key to improved weather prediction. *Jour. Roy. Meteor. Soc.*, **117**, 267-297.
- _____, Woolf, H. M., Nieman, S. J., and T. H. Achtor, 1993: ITPP-5 - The use of AVHRR and TIGR in TOVS Data Processing. Technical Proceedings of the Seventh International TOVS Study Conference held in Igls, Austria 10 to 16 February 1993, J. R. Eyre Ed., 443-453.
- Sullivan, J., Gandin, L., Gruber, A., and W. Baker, 1993: Observation Error Statistics for NOAA-10 Temperature and Height Retrievals. *Mon. Wea. Rev.*, **121**, 2578-2587.
- Twomey, S., 1977: An introduction to the mathematics of inversion in remote sensing and indirect measurements. Elsevier, New York.
- Wark, D. Q., 1961: On indirect temperature soundings of the stratosphere from satellites. *J. Geophys. Res.*, **66**, 77.
- _____, Hilleary, D.T., Anderson, S. P., and J. C. Fisher, 1970: Nimbus satellite infrared spectrometer experiments. *IEEE. Trans. Geosci. Electron.*, **GE-8**, 264-270.